IOP Publishing Journal of Physics: Condensed Matter
J. Phys.: Condens. Matter 29 (2017) 475201 (6pp) https://doi.org/10.1088/1361-648X/aa92fe

Statistical analysis of the reduction process of graphene oxide probed by Raman spectroscopy mapping

A Wróblewska[1], A Dużyńska[1], J Judek[1], L Stobiński[2], K Żerańska[1], A P Gertych[1] and M Zdrojek[1]

[1] Faculty of Physics, Warsaw University of Technology, Koszykowa 75, 00-662 Warsaw, Poland
[2] Faculty of Chemical and Process Engineering, Warsaw University of Technology, Warynskiego 1, Warsaw, Poland

E-mail: zdrojek@if.pw.edu.pl

Received 5 July 2017, revised 10 October 2017
Accepted for publication 12 October 2017
Published 3 November 2017

Abstract

We propose a method for monitoring the large-scale homogeneity of the reduction process of graphene oxide. For this purpose, a Raman mapping technique is employed to probe the evolution of the phonon properties of two different graphene oxide (GO) thin films upon controllable thermal reduction. The reduction of GO is reflected by the upshift of the statistical distribution of the relative intensity ratio of the G and D peaks (I_D/I_G) of the Raman spectra and is consistent with the ratio obtained for chemically reduced GO. In addition, the shifts of the position distributions of the main Raman modes (ω_D, ω_G) and their cross-correlation with the I_D/I_G ratio provides evidence of a change of the doping level, demonstrating the influence of reduction processes on GO films.

Keywords: graphene oxide, reduced graphene oxide, Raman spectroscopy, reduction process monitoring

(Some figures may appear in colour only in the online journal)

1. Introduction

Graphene oxide (GO) is a carbon-based material containing a hexagonal-like structure with both sp^2 and sp^3 hybridization and enriched by many different functional groups (mainly oxygen). GO is synthesized by an oxidation process of graphite using variations of basic methods such as those of Staudenmaier, Hofmann, Brodie and Hummers [1]. GO has properties very different from those of pristine graphene due to the disrupted sp^2 bonds. However, it is possible to restore the π-network structure employing reduction reactions. Thus, GO is very often used as a starting point for production of graphene flakes or reduced graphene oxide (rGO) flakes [2].

The oxidation level (sp^2 to sp^3 ratio, oxygen to carbon content) of GO or rGO strongly influences the electronic, optical and chemical properties, and it is crucial for their applications. For example, GO is an insulator but rGO is a good conductor [3], and the optical absorption of rGO resembles that of graphene, in contrast to GO [4]. All these properties can be tuned by controlling the oxidation level of graphene oxide, especially by the reduction process, thus allowing for many types of practical applications. Depending on the oxidation level, a graphene oxide can be used for biosensing or drug delivery platforms [5, 6], energy or hydrogen storage [7, 8], solar cell unit cells [9], transparent electrodes [10] or water filtration technology [11].

To determine whether graphene oxide can be used in any of these applications the oxidation level or the effectiveness of the reduction process must be known, and thus the quality of the obtained material. Raman spectroscopy is a powerful technique for this purpose that has already been widely used to study the properties of carbon nanostructures including graphene [12], GO and rGO [13].

 © 2017 IOP Publishing Ltd Printed in the UK

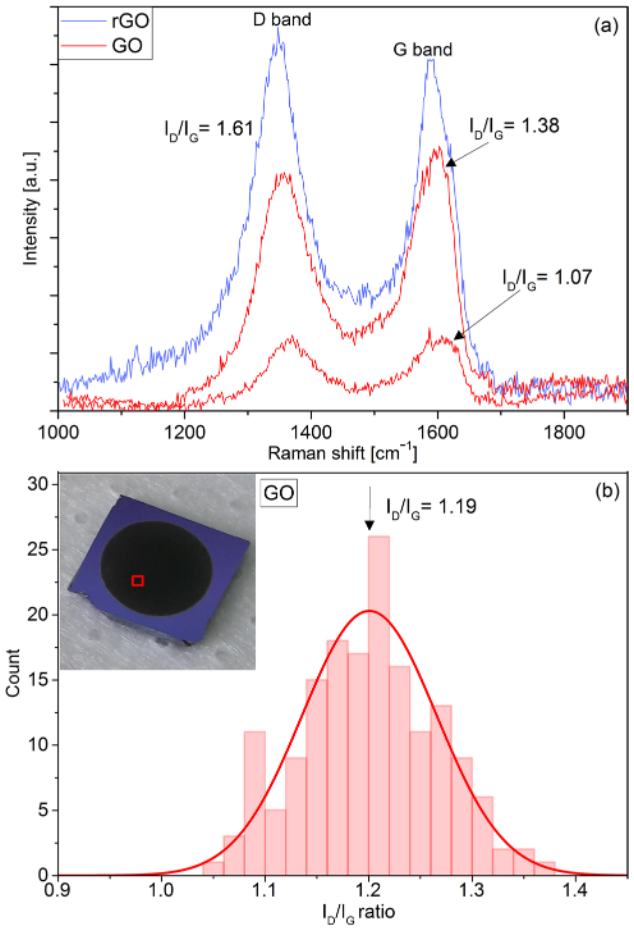

Figure 1. (a) Single Raman spectra of graphene oxide (sample A) taken at two places on the sample indicating significantly different I_D/I_G ratios. The reduced GO spectrum is also shown for comparison. (b) Histograms of the I_D/I_G ratio with a mean value of 1.19 extracted from a Raman map on the sample shown in the inset (GO film diameter is ~1 cm). The histogram is fit with a Gaussian line with width at half maximum of ~0.12.

The Raman technique has been used, for instance, to monitor the evolution of the structure of graphite oxide upon thermal reduction [14, 15], to show how the reduction process modifies the electrical conductivity of the GO thin films [16], and to demonstrate the 'repair of defects' effect in rGO films upon proper graphitization [17]. A Raman study relies on an analysis of the main Raman peaks in the spectra of graphene material (D, G and 2D), their position, width and especially the relative intensity ratio—I_D/I_G (an increase in I_D/I_G reflects a reduction of the oxidation level [15]).

The G band in the Raman spectra corresponds to sp^2 hybridized carbon-based material [18]. The D peak is related to defects or lattice disorder due to oxygen-functional group binding [12, 19]. The intensity of the D band is associated with the size of the sp^2 in-plane domains, and thus increases for rGO [18], which can be seen in figure 1(a) (black curve versus blue curve—GO versus rGO). According to the literature [17, 20] our GO samples are in the regime (classified as nanocrystalline graphene stage) where the mean defects distance L_a is low (~10 nm).

Of note in the literature is that the I_D/I_G ratio used to identify GO and rGO in Raman spectroscopy is in a wide range of 0.67–1.4 and 0.91–1.9, respectively [17, 21–34](see also table 1), which often makes the comparison of graphene materials difficult, and needs to be carefully considered. The ratio might also depend on the laser wavelength used in the Raman study (see table 1). Additionally, quite often, only single point measurement spectra are taken and are used to identify GO or rGO [24, 35], which could introduce additional uncertainty in I_D/I_G peak intensity ratio. This suggests that a statistical analysis of the quality of graphene oxide materials using Raman spectroscopy is needed.

In this work, we propose an approach based on Raman mapping for statistical analysis of Raman features obtained from large area GO and rGO thin films. This approach gives global and reliable information about the homogeneity of the oxidation level, and the quality or purity of GO/rGO material. We demonstrate that using histograms of I_D/I_G and other peak parameter correlations (both produced from Raman maps), one can monitor the changes during gradual thermal reduction of GO. In addition, statistical cross-correlation of peak parameters (I_D/I_G versus peaks position) shows the evident influence of changes in the doping level of GO on the reduction process.

2. Results and discussion

The graphene oxide material used in this work was acquired from two different commercial sources (Nanomaterials LS, Poland, and Graphenea, Spain), which for simplicity we call provider A and B, respectively. In both cases, GO was prepared via the modified Hummers method (according to the manufacturer's specification). In addition, GO obtained from Nanomaterials LS was reduced with hydrazine [36] and it was further used as a reference for other samples. All samples were prepared in the same way, via drop casting of deionized water based solution with 2 mg ml^{-1} of graphene material. A solution of graphene material was left to dry on the substrate (Si/SiO_2) at room temperature, forming thin films of GO or rGO. The thickness and the size of the films were the same (verified by AFM, data not shown).

Raman spectra were collected using a Renishaw inVia spectrometer with a 514 nm laser source and an x50 microscope objective (laser spot ~2 μm). The experiment was conducted at room temperature. To avoid heating of the sample, the laser power was kept low (<0.3 mW, calibrated on the samples). The Raman mapping mode was used with a scan area of approximately 50 μm × 50 μm, containing 250 spectra. Each spectrum (figure 1(a)), consisting of two main bands, a G band (~1600 cm^{-1}) and a D band (~1350 cm^{-1}), was fit using a Lorentzian line shape. The parameters obtained from the fitting procedure (relative intensity, position and width) for each peak of a given map were afterwards presented as a histogram. The resolution of peak position determination was ~0.5 cm^{-1}.

First, we demonstrated the difference between single point spectra and a statistical Raman map, and the consequences this has on results interpretation, using the following example.

Table 1. Comparison of selected Raman peak intensity ratios (I_D/I_G) for GO and rGO obtained for different excitation laser wavelengths. All GO samples have been prepared via the modified Hummers method and for rGO different methods have been applied.

		Intensity ratio (I_D/I_G)		
	λ (nm)	GO	rGO	Reduction method
Chang [21]	458	0.67	—	—
Kim [22]	—	0.86	—	—
Konios [23]	—	0.90	1.10	Chemical
Dai [24]	—	0.91	0.91/0.95	Photocatalytic
Wu [25]	532	0.95	—	—
Rajagopalan [26]	633	1.1	—	—
Shao [27]	515	1.00	1.42	NH_2OH
Kim [28]	—	1.09	0.98/1.02/1.13	Plasma exposure
Kaniyoor [29]	532	1.10	—	—
Matsumoto [30]	532	1.12	0,98	Photoreduction H_2
			0.96/1.02	Photoreduction H_2/N_2
			1.20	Hydrazine hydrate
Eigler [31]	532	1.14/1.19	1.28/2.70	Hydrazine hydrate
Chen [32]	633	1.16	1.30/1.44	$H_2SO_4/MnCl_2/NaBH_4/AlCl_3$
			1.47/1.48	
This work	514	1.21/1.29	1.43	Hydrazine hydrate
			1.33 → 1.50	Temperature
Fu [33]	514	1.37	1.15	Temperature
Boutchich [34]	532	1.40	1.55	Microorganisms
			1.60	UV photocatalysis
			1.90	Hydrazine hydrate
Rozada [17]	532	1.83		

Figure 1(a) shows two Raman spectra (red curves) of GO collected (within one map) in a randomly chosen area of the sample (see inset of figure 1(b)). The value of the relative intensity I_D/I_G for both spectra are quite different (1.38 versus 1.07), even though the spectra were collected only a dozen micrometers from each other. This may suggest the interpretation that our graphene oxide film is not uniform or that more rGO than GO is present at one point. In both cases, the global interpretation is not clear. However, if we consider the entire map (250 spectra, red area marked on the sample, in the inset picture) and look at the distribution of the I_D/I_G ratio (histogram in figure 1(b)) we see that both values considered as a single spectrum are here the extreme values of one distribution, and the mean value is 1.19. We note that, if we collect another map from another part of the sample, the corresponding histogram of the I_D/I_G ratio has a very similar distribution. The above example shows that the level of homogeneity of our graphene oxide sample is not high, and suggests that the mean value of the histogram is a more reliable representation of the general condition of the sample compared to a single spectral measurement. Consequently, this approach can be used to study the homogeneity of any GO/rGO samples, which would be reflected in a much different histogram distribution (mean value, and FWHM).

Now we consider the possibility of using the Raman mapping method to monitor the structure evolution from graphene oxide to reduced graphene oxide. In this work, we use thermal annealing to conduct the reduction process. Most of the functional groups (attached to the graphene surface) can be removed upon thermal heating [37]. To demonstrate the change in the GO structure (sample A) upon heating, we took an untreated sample (represented by the red histogram in figure 2(a), $I_D/I_G = 1.21$) and kept it in an oven at 100 °C (in ambient atmosphere and pressure) for 72 h. Every 24 h the sample was removed from the oven (for max. 1 h) and Raman spectra were collected. As seen in figure 2(a), the first heating period caused a shift of the I_D/I_G ratio from 1.21 to 1.33, as expected (due to the thermal removal of functional groups). This effect is consistent with the literature [35]. Subsequent heating periods caused a further but less significant shift of the ratio (up to 1.37). Therefore, the most intense reduction process occurred within the first 24 h. We note that the magnitude of the shift depends on the temperature and heating time, as demonstrated previously [38], but we do not discuss this issue in this work. Here, we have shown that thermal reduction of GO and its effectiveness can be easily controlled by statistical Raman mapping.

The increase of the intensity ratio I_D/I_G is related to the decrease of the crystalline domain size L_a (here, from 3.64 nm to 3.07 nm according to [18] and considering obtained ratio values). This effect is due to the increased disorder structure introduced by the reduction process.

The same graphene oxide material used in the annealing process was also subjected to the reduction process using hydrazine, which is very common way to obtain rGO [36]. We use hydrazine reduced GO as a benchmark for thermally reduced graphene in the Raman study, and the histogram of the I_D/I_G ratio corresponding to this sample is shown in figure 2(a) (in blue). The mean value of the histogram (from a Gaussian fit) is 1.43, which is only slightly more than that of the thermally reduced GO sample (1.38). This shows that

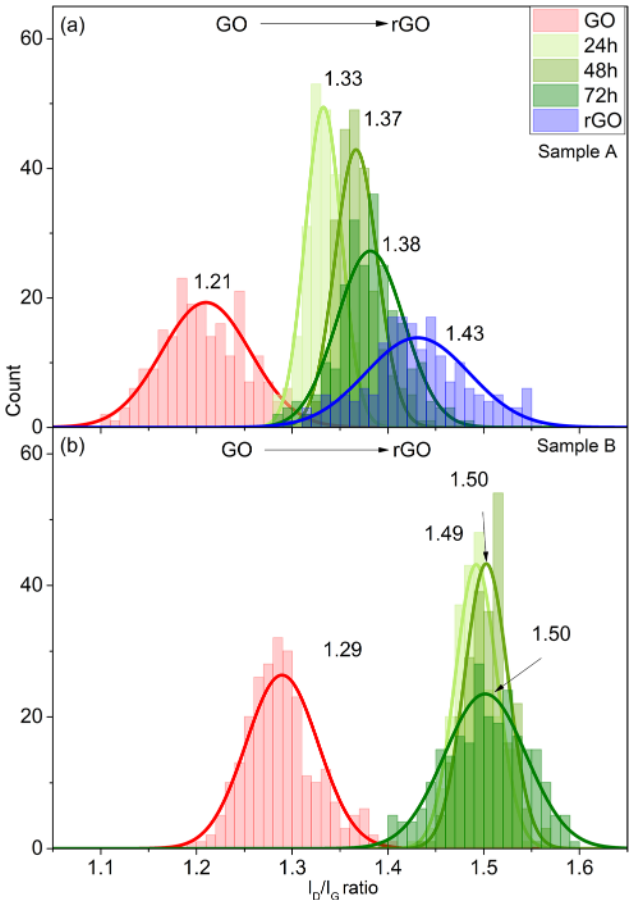

Figure 2. (a) Evolution of the I_D/I_G ratio of GO upon thermal reduction for sample A. Red histogram (mean 1.21, $\sigma \sim 0.1$) is the reference data obtained for the unheated sample. For comparison, the blue histogram (1.43) comes from GO reduced by hydrazine. (b) The I_D/I_G ratio of GO upon thermal reduction for sample B. The solid lines in all histograms correspond to a Gaussian fit to the data.

the thermal reduction process can be as efficient as chemical reduction (hydrazine) and can be seen in Raman signatures.

We further validated the Raman statistical analysis of graphene oxide using the material from sample B (Graphenea). The corresponding histogram of the I_D/I_G ratio is shown in figure 2(b), with a mean value of 1.29 that is reproducible within the sample (data not shown). Note that the initial value is slightly bigger than that of the sample A sample, suggesting a slight difference in structure between samples. Next, the material was subjected to thermal reduction under identical conditions as before. There are significant changes in the results compared to data shown in figure 2(a). First, after 24 h of annealing, the shift of the I_D/I_G ratio is much bigger (1.29 → 1.49) suggesting that the reduction process for this material is much faster. Second, the subsequent heating periods have no effect on further reduction of GO (I_D/I_G is not changed). This is probably due to the relatively low temperature (100 °C) used for thermal annealing. The increased temperature could speed up the process and also cause it more effective within given time.

The other parameters of the Raman spectra that are sensitive to the structure of graphene oxide are the positions of the D and G bands. The histograms of those parameters (ω_D and ω_G) for both types of GO samples subjected to thermal reduction (discussed in figure 2) are plotted in figure 3. For both GO samples similar trends in shifts as a function of the reduction level are observed. The position of the G peak shifts towards higher energy ($h\omega_{D,G}$), but the shift is less pronounced for the sample A. The position of the D band shifts towards lower energy. Additionally, for comparison, the ω_D and ω_G parameters for GO reduced with hydrazine are shown in figures 3(a) and (b) and are consistent with parameter evolution during thermal reduction.

The G peak position change is related to structural disorder [17] and more often to doping [39, 40]. The position of G increases for both electron and hole doping (due to the non-adiabatic removal of the Kohn anomaly [41]). The reduction process (thermal or wet) removed the oxygen groups, causing an increase in the doping level [40], which is manifested by the stiffening of the G mode position (seen in figures 3(a) and (c)). The level of doping also strongly influences the D peak position [40, 42, 43]. The increase of electron doping caused a downshift of the peak position, which can be observed in figures 3(b) and (d). Additionally, we can exclude the stress/tension effect upon heating/cooling as a primary contribution for peak shifts because samples were treated at relatively low temperature and several series of samples have been prepared showing no difference with respect to the given thermal reduction stage.

Finally, we show the cross-correlation of the I_D/I_G ratio versus the G peak position for two different GO material sources. The corresponding scatter plots are shown in figure 4, where the dotted lines are a visual guide for showing the doping trend changes during the reduction process and compared with the hydrazine reduced GO (only for provider A, circle blue dots). Figures 4(a) and (b) show that trends of the I_D/I_G ratio with respect to ω_G and ω_D positions for both types of samples are consistent with the data shown in figures 2 and 3 (increase of the ratio for ω_G upshift and ω_D downshift), and reflect the change in the doping level upon functional group removal due to the reduction process. In addition, this correlation agrees with the study of defected graphene as a function of doping demonstrated by Bruno *et al* [40]. Another indication of doping change is a clear correlation between the G mode width decrease and the shift of its position to higher energy (figures 4(c) and (d)) which is a result of variation in electron concentration in the graphene structure. A similar effect has been observed for single layer graphene [44–46] and for carbon nanotubes [47]. Finally, the relation of the two main peak positions (ω_D, ω_G, figures 4(e) and (f)) are correlated with histograms for different reduction process steps (shown in figures 2 and 3) and evidently shows trends upon change of doping [48, 49].

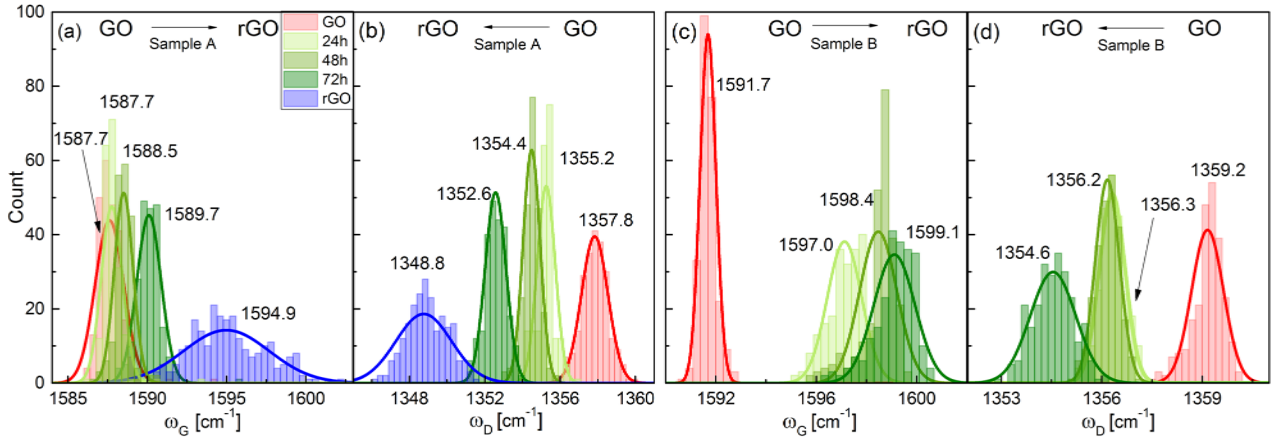

Figure 3. Raman peak position distributions (with mean values indicated) as a function of the thermal reduction process for (a) the G peak and (b) the D peak, for sample A. For comparison, hydrazine-reduced rGO is shown (blue histogram). (c) The histogram of G peak and (d) D peak positions for sample B. Arrows show the direction of peak shifts upon reduction. The solid lines correspond to a Gaussian fit to the data.

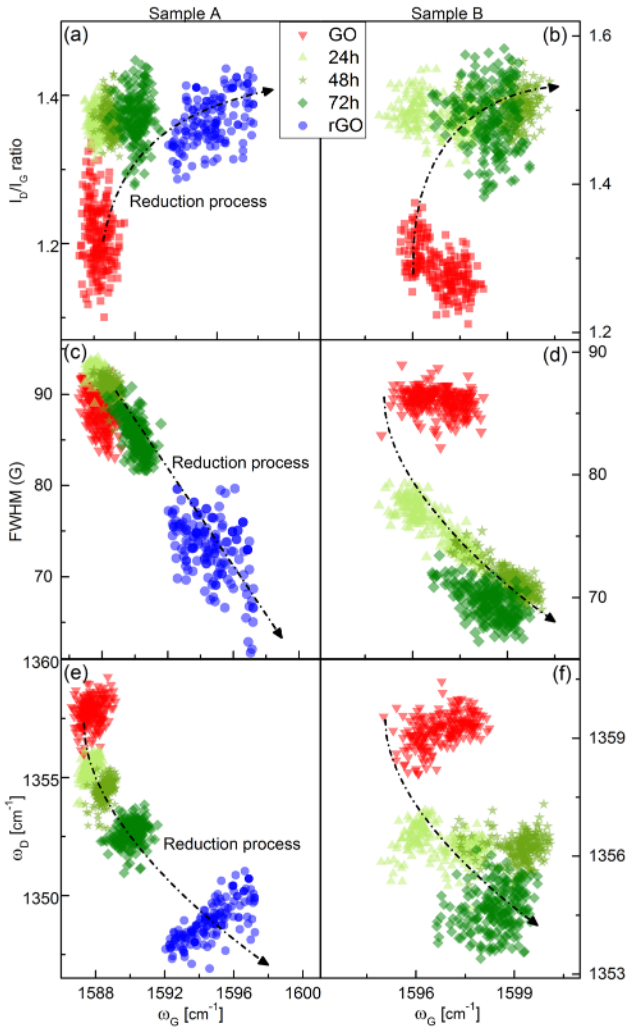

Figure 4. The I_D/I_G ratio versus (a) G peak position and (b) D peak position, both for GO samples (provider A) upon thermal reduction. Similarly, for provider B, the I_D/I_G ratio versus (c) G peak position and (d) D peak position. The dotted lines are a visual guide for showing the trend changes.

3. Conclusions

In conclusion, we have performed a systematic and statistical study of the phonon behavior of graphene oxide and reduced graphene oxide thin films with the Raman mapping technique. We showed that for proper determination of the uniformity of the GO material, a statistical analysis of the I_D/I_G ratio should be used. Importantly, the I_D/I_G ratio can be used to monitor the reduction process that results in functional group removal and thus changes the doping level. The statistical position of the D and G modes, and their cross-correlation with the I_D/I_G ratio also show the evidence of change in the reduction level of GO/rGO films.

Acknowledgments

JJ and AG thank the National Science Centre, Poland, for support in Project No. 2014/15/D/ST5/03944. This work was supported by Foundation for Polish Science under the TEAM-TECH programme (TEAM-TECH/2016-3/21).

ORCID iDs

J Judek https://orcid.org/0000-0002-4326-7392
M Zdrojek https://orcid.org/0000-0002-8897-6205

References

[1] Dreyer D R, Park S, Bielawski C W and Ruoff R S 2009 *Chem. Soc. Rev.* **39** 228
[2] Tung T T, Yoo J, Alotaibi F K, Nine M J, Karunagaran R, Krebsz M, Nguyen G T, Tran D N H, Feller J-F and Losic D 2016 *ACS Appl. Mater. Interfaces* **8** 16521
[3] Eda G, Mattevi C, Yamaguchi H, Kim H and Chhowalla M 2009 *J. Phys. Chem.* C **113** 15768
[4] Li B, Zhang X, Chen P, Li X, Wang L, Zhang C, Zheng W and Liu Y 2013 *RSC Adv.* **4** 2404

[5] Lu C-H, Yang H-H, Zhu C-L, Chen X and Chen G-N 2009 *Angew. Chem., Int. Ed. Engl.* **48** 4785
[6] Liu Z, Robinson J T, Sun X and Dai H 2008 *J. Am. Chem. Soc.* **130** 10876
[7] Zhou W, Liu J, Chen T, Tan K S, Jia X, Luo Z, Cong C, Yang H, Li C M and Yu T 2011 *Phys. Chem. Chem. Phys.* **13** 14462
[8] Wang L, Lee K, Sun Y-Y, Lucking M, Chen Z, Zhao J J and Zhang S B 2009 *ACS Nano* **3** 2995
[9] Wu Z, Bai S, Xiang J, Yuan Z, Yang Y, Cui W, Gao X, Liu Z, Jin Y and Sun B 2014 *Nanoscale* **6** 10505
[10] Becerril H A, Mao J, Liu Z, Stoltenberg R M, Bao Z and Chen Y 2008 *ACS Nano* **2** 463
[11] Hu M and Mi B 2013 *Environ. Sci. Technol.* **47** 3715
[12] Ferrari A C and Basko D M 2013 *Nat. Nanotechnol.* **8** 235
[13] Tokarczyk M, Kowalski G, Witowski A, Kozinski R, Librant K, Aksienionek M, Lipinska L and Ciepielewski P 2014 *Acta Phys. Pol.* A **126** 1190
[14] Zhan D, Ni Z, Chen W, Sun L, Luo Z, Lai L, Yu T, Wee A T S and Shen Z 2011 *Carbon* **49** 1362
[15] Sahoo M, Antony R P, Mathews T, Dash S, Tyagi A K, Chauhan A K, Murli C and Gadkari S C 2013 *AIP Conf. Proc.* **1512** 1262
[16] Díez-Betriu X, Álvarez-García S, Botas C, Álvarez P, Sánchez-Marcos J, Prieto C, Menéndez R and de Andrés A 2013 *J. Mater. Chem.* C **1** 6905
[17] Rozada R, Paredes J I, Villar-Rodil S, Martínez-Alonso A and Tascón J M D 2013 *Nano Res.* **6** 216
[18] Ferrari A C and Robertson J 2000 *Phys. Rev.* B **61** 14095
[19] Dzukarnain M Z B, Takami T, Imai H and Ogino T 2016 *Thin Solid Films* **615** 247
[20] Grimm S, Schweiger M, Eigler S and Zaumseil J 2016 *J. Phys. Chem.* C **120** 3036
[21] Chang L, Wu S, Chen S and Li X 2011 *J. Mater. Sci.* **46** 2024
[22] Kim S-G, Park O-K, Lee J H and Ku B-C 2013 *Carbon Lett.* **14** 247
[23] Konios D, Stylianakis M M, Stratakis E and Kymakis E 2014 *J. Colloid Interface Sci.* **430** 108
[24] Dai Y, Jing Y, Zeng J, Qi Q, Wang C, Goldfeld D, Xu C, Zheng Y and Sun Y 2011 *J. Mater. Chem.* **21** 18174
[25] Wu T, Gao J, Xu X, Wang W, Gao C and Qiu H 2013 *Nanotechnology* **24** 215604
[26] Rajagopalan B and Chung J S 2014 *Nanoscale Res. Lett.* **9** 535
[27] Shao D, Li J and Wang X 2014 *Sci. China Chem.* **57** 1449
[28] Kim M J, Jeong Y, Sohn S, Lee S Y, Kim Y J, Lee K, Kahng Y H and Jang J-H 2013 *AIP Adv.* **3** 012117
[29] Kaniyoor A and Ramaprabhu S 2012 *AIP Adv.* **2** 032183
[30] Matsumoto Y, Koinuma M, Kim S Y, Watanabe Y, Taniguchi T, Hatakeyama K, Tateishi H and Ida S 2010 *ACS Appl. Mater. Interfaces* **2** 3461
[31] Eigler S, Dotzer C and Hirsch A 2012 *Carbon* **50** 3666
[32] Chen C, Chen T, Wang H, Sun G and Yang X 2011 *Nanotechnology* **22** 405602
[33] Fu C, Zhao G, Zhang H and Li S 2013 *Int. J. Electrochem. Sci.* **8** 6269
[34] Boutchich M *et al* 2013 *J. Phys.: Conf. Ser.* **433** 012001
[35] King A A K, Davies B R, Noorbehesht N, Newman P, Church T L, Harris A T, Razal J M and Minett A I 2016 *Sci. Rep.* **6** 19491
[36] Stobinski L, Lesiak B, Malolepszy A, Mazurkiewicz M, Mierzwa B, Zemek J, Jiricek P and Bieloshapka I 2014 *J. Electron Spectrosc. Relat. Phenom.* **195** 145
[37] Tegou E, Pseiropoulos G, Filippidou M K and Chatzandroulis S 2016 *Microelectron. Eng.* **159** 146
[38] Kimiagar S, Rashidi N and Ghadim E E 2015 *Bull. Mater. Sci.* **38** 1699
[39] Das A *et al* 2008 *Nat. Nanotechnol.* **3** 210
[40] Bruna M, Ott A K, Ijäs M, Yoon D, Sassi U and Ferrari A C 2014 *ACS Nano* **8** 7432
[41] Lazzeri M and Mauri F 2006 *Phys. Rev. Lett.* **97** 266407
[42] Ott A, Verzhbitskiy I A, Clough J, Eckmann A, Georgiou T and Casiraghi C 2014 *Nano Res.* **7** 338
[43] Liu J, Li Q, Zou Y, Qian Q, Jin Y, Li G, Jiang K and Fan S 2013 *Nano Lett.* **13** 6170
[44] Casiraghi C, Pisana S, Novoselov K S, Geim A K and Ferrari A C 2007 *Appl. Phys. Lett.* **91** 233108
[45] Pisana S, Lazzeri M, Casiraghi C, Novoselov K S, Geim A K, Ferrari A C and Mauri F 2007 *Nat. Mater.* **6** 198
[46] Shim J, Lui C H, Ko T Y, Yu Y-J, Kim P, Heinz T F and Ryu S 2012 *Nano Lett.* **12** 648
[47] Paulus G L C, Wang Q H, Ulissi Z W, McNicholas T P, Vijayaraghavan A, Shih C-J, Jin Z and Strano M S 2013 *Small* **9** 1954
[48] Wang Q H *et al* 2012 *Nat. Chem.* **4** 724
[49] Krishnamoorthy K, Veerapandian M, Yun K and Kim S-J 2013 *Carbon* **53** 38